

SUPPLEMENTAL INFORMATION

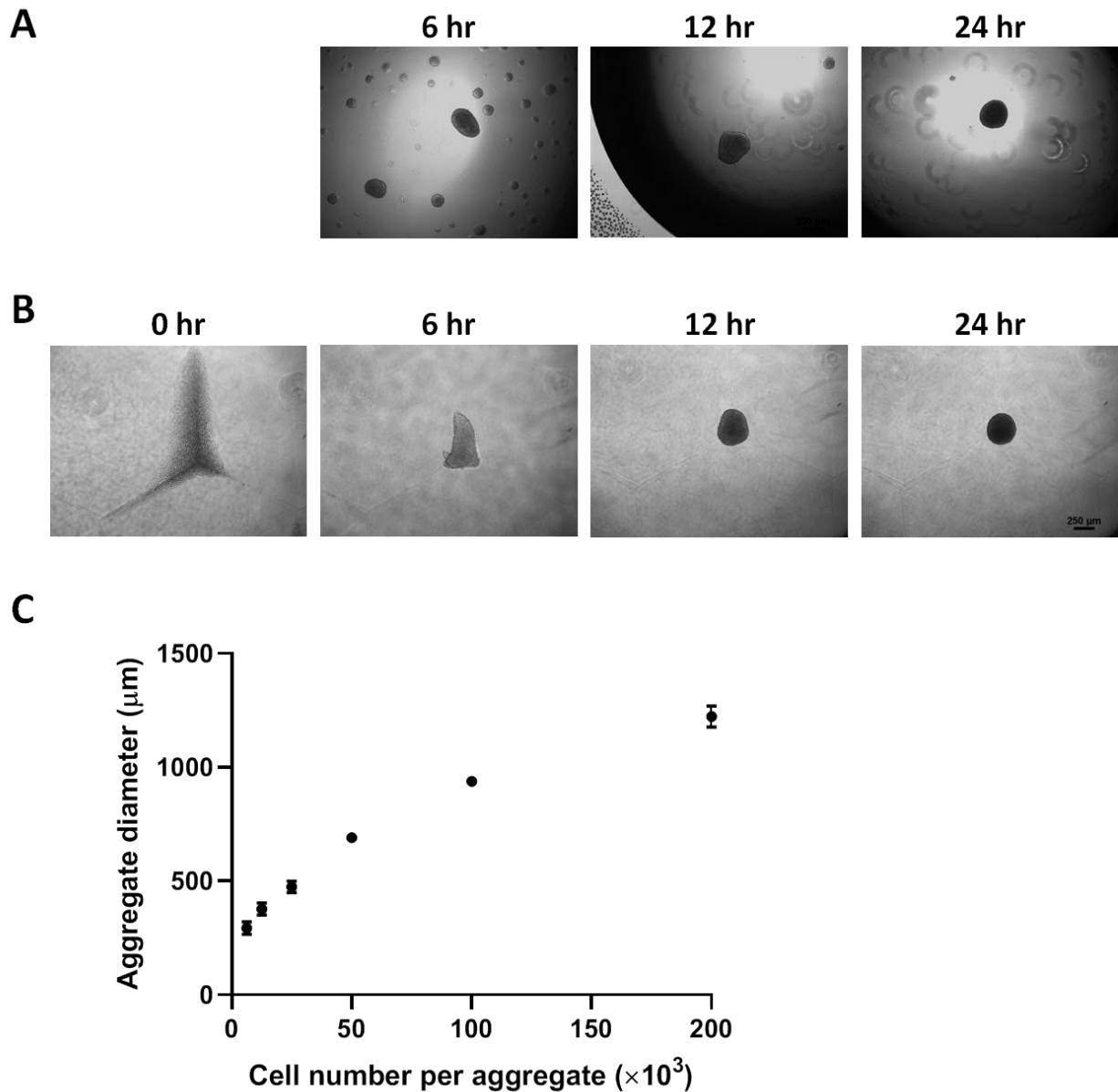
Supplementary Table S1. List of genes for RT2 Profiler qPCR Array – Human Mesenchymal Stem Cells.

UniGene	GenBank	Gene Symbol	Description
Hs.489033	NM_000927	ABCB1	ATP-binding cassette, sub-family B (MDR/TAP), member 1
Hs.500483	NM_001613	ACTA2	Actin, alpha 2, smooth muscle, aorta
Hs.591293	NM_001627	ALCAM	Activated leukocyte cell adhesion molecule
Hs.1239	NM_001150	ANPEP	Alanyl (membrane) aminopeptidase
Hs.480653	NM_001154	ANXA5	Annexin A5
Hs.502182	NM_001709	BDNF	Brain-derived neurotrophic factor
Hs.654541	NM_199173	BGLAP	Bone gamma-carboxyglutamate (gla) protein
Hs.73853	NM_001200	BMP2	Bone morphogenetic protein 2
Hs.68879	NM_130851	BMP4	Bone morphogenetic protein 4
Hs.285671	NM_001718	BMP6	Bone morphogenetic protein 6
Hs.473163	NM_001719	BMP7	Bone morphogenetic protein 7
Hs.141125	NM_004346	CASP3	Caspase 3, apoptosis-related cysteine peptidase
Hs.502328	NM_000610	CD44	CD44 molecule (Indian blood group)
Hs.172928	NM_000088	COL1A1	Collagen, type I, alpha 1
Hs.1349	NM_000758	CSF2	Colony stimulating factor 2 (granulocyte-macrophage)
Hs.2233	NM_000759	CSF3	Colony stimulating factor 3 (granulocyte)
Hs.476018	NM_001904	CTNNB1	Catenin (cadherin-associated protein), beta 1, 88kDa
Hs.419815	NM_001963	EGF	Epidermal growth factor
Hs.76753	NM_000118	ENG	Endoglin
Hs.446352	NM_004448	ERBB2	V-erb-b2 erythroblastic leukemia viral oncogene homolog 2, neuro/glioblastoma derived oncogene homolog (avian)
Hs.664499	NM_004465	FGF10	Fibroblast growth factor 10
Hs.284244	NM_002006	FGF2	Fibroblast growth factor 2 (basic)
Hs.69747	NM_000148	FUT1	Fucosyltransferase 1 (galactoside 2-alpha-L-fucosyltransferase, H blood group)
Hs.390420	NM_002033	FUT4	Fucosyltransferase 4 (alpha (1,3) fucosyltransferase, myeloid-specific)
Hs.647029	NM_003508	FZD9	Frizzled family receptor 9
Hs.616962	NM_004864	GDF15	Growth differentiation factor 15
Hs.1573	NM_000557	GDF5	Growth differentiation factor 5
Hs.492277	NM_001001557	GDF6	Growth differentiation factor 6
Hs.447688	NM_182828	GDF7	Growth differentiation factor 7

Hs.445977	NM_002097	GTF3A	General transcription factor IIIA
Hs.632532	NM_003642	HAT1	Histone acetyltransferase 1
Hs.88556	NM_004964	HDAC1	Histone deacetylase 1
Hs.396530	NM_000601	HGF	Hepatocyte growth factor (hepapoietin A; scatter factor)
Hs.654455	NM_000545	HNF1A	HNF1 homeobox A
Hs.643447	NM_000201	ICAM1	Intercellular adhesion molecule 1
Hs.856	NM_000619	IFNG	Interferon, gamma
Hs.160562	NM_000618	IGF1	Insulin-like growth factor 1 (somatomedin C)
Hs.193717	NM_000572	IL10	Interleukin 10
Hs.126256	NM_000576	IL1B	Interleukin 1, beta
Hs.654458	NM_000600	IL6	Interleukin 6 (interferon, beta 2)
Hs.654579	NM_000207	INS	Insulin
Hs.133397	NM_000210	ITGA6	Integrin, alpha 6
Hs.436873	NM_002210	ITGAV	Integrin, alpha V (vitronectin receptor, alpha polypeptide, antigen CD51)
Hs.248472	NM_000887	ITGAX	Integrin, alpha X (complement component 3 receptor 4 subunit)
Hs.643813	NM_002211	ITGB1	Integrin, beta 1 (fibronectin receptor, beta polypeptide, antigen CD29 includes MDF2, MSK12)
Hs.728907	NM_000214	JAG1	Jagged 1
Hs.533055	NM_003884	KAT2B	K(lysine) acetyltransferase 2B
Hs.479756	NM_002253	KDR	Kinase insert domain receptor (a type III receptor tyrosine kinase)
Hs.1048	NM_003994	KITLG	KIT ligand
Hs.2250	NM_002309	LIF	Leukemia inhibitory factor (cholinergic differentiation factor)
Hs.599039	NM_006500	MCAM	Melanoma cell adhesion molecule
Hs.513617	NM_004530	MMP2	Matrix metalloproteinase 2 (gelatinase A, 72kDa gelatinase, 72kDa type IV collagenase)
Hs.527971	NM_006617	NES	Nestin
Hs.415768	NM_002507	NGFR	Nerve growth factor receptor
Hs.495473	NM_017617	NOTCH1	Notch 1
Hs.153952	NM_002526	NT5E	5'-nucleotidase, ecto (CD73)
Hs.558459	NM_007083	NUDT6	Nudix (nucleoside diphosphate linked moiety X)-type motif 6
Hs.509067	NM_002609	PDGFRB	Platelet-derived growth factor receptor, beta polypeptide
Hs.462550	NM_033198	PIGS	Phosphatidylinositol glycan anchor biosynthesis, class S
Hs.249184	NM_002701	POU5F1	POU class 5 homeobox 1
Hs.162646	NM_015869	PPARG	Peroxisome proliferator-activated receptor gamma

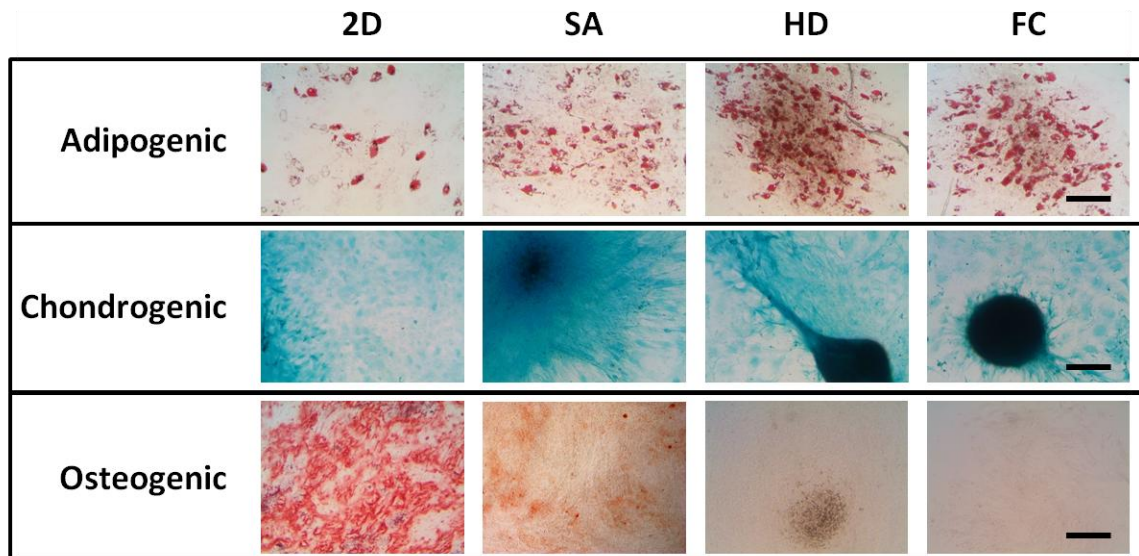
Hs.614734	NM_006017	PROM1	Prominin 1
Hs.395482	NM_005607	PTK2	PTK2 protein tyrosine kinase 2
Hs.654514	NM_002838	PTPRC	Protein tyrosine phosphatase, receptor type, C
Hs.247077	NM_001664	RHOA	Ras homolog gene family, member A
Hs.535845	NM_004348	RUNX2	Runt-related transcription factor 2
Hs.597422	NM_012434	SLC17A5	Solute carrier family 17 (anion/sugar transporter), member 5
Hs.75862	NM_005359	SMAD4	SMAD family member 4
Hs.189329	NM_020429	SMURF1	SMAD specific E3 ubiquitin protein ligase 1
Hs.705442	NM_022739	SMURF2	SMAD specific E3 ubiquitin protein ligase 2
Hs.518438	NM_003106	SOX2	SRY (sex determining region Y)-box 2
Hs.647409	NM_000346	SOX9	SRY (sex determining region Y)-box 9
Hs.381715	NM_181486	TBX5	T-box 5
Hs.492203	NM_198253	TERT	Telomerase reverse transcriptase
Hs.645227	NM_000660	TGFB1	Transforming growth factor, beta 1
Hs.592317	NM_003239	TGFB3	Transforming growth factor, beta 3
Hs.644697	NM_006288	THY1	Thy-1 cell surface antigen
Hs.241570	NM_000594	TNF	Tumor necrosis factor
Hs.109225	NM_001078	VCAM1	Vascular cell adhesion molecule 1
Hs.73793	NM_003376	VEGFA	Vascular endothelial growth factor A
Hs.642813	NM_003380	VIM	Vimentin
Hs.440848	NM_000552	VWF	Von Willebrand factor
Hs.336930	NM_033131	WNT3A	Wingless-type MMTV integration site family, member 3A
Hs.335787	NM_174900	ZFP42	Zinc finger protein 42 homolog (mouse)
Hs.520640	NM_001101	ACTB	Actin, beta
Hs.534255	NM_004048	B2M	Beta-2-microglobulin
Hs.592355	NM_002046	GAPDH	Glyceraldehyde-3-phosphate dehydrogenase
Hs.412707	NM_000194	HPRT1	Hypoxanthine phosphoribosyltransferase 1
Hs.546285	NM_001002	RPLP0	Ribosomal protein, large, P0

SUPPLEMENTARY FIGURES

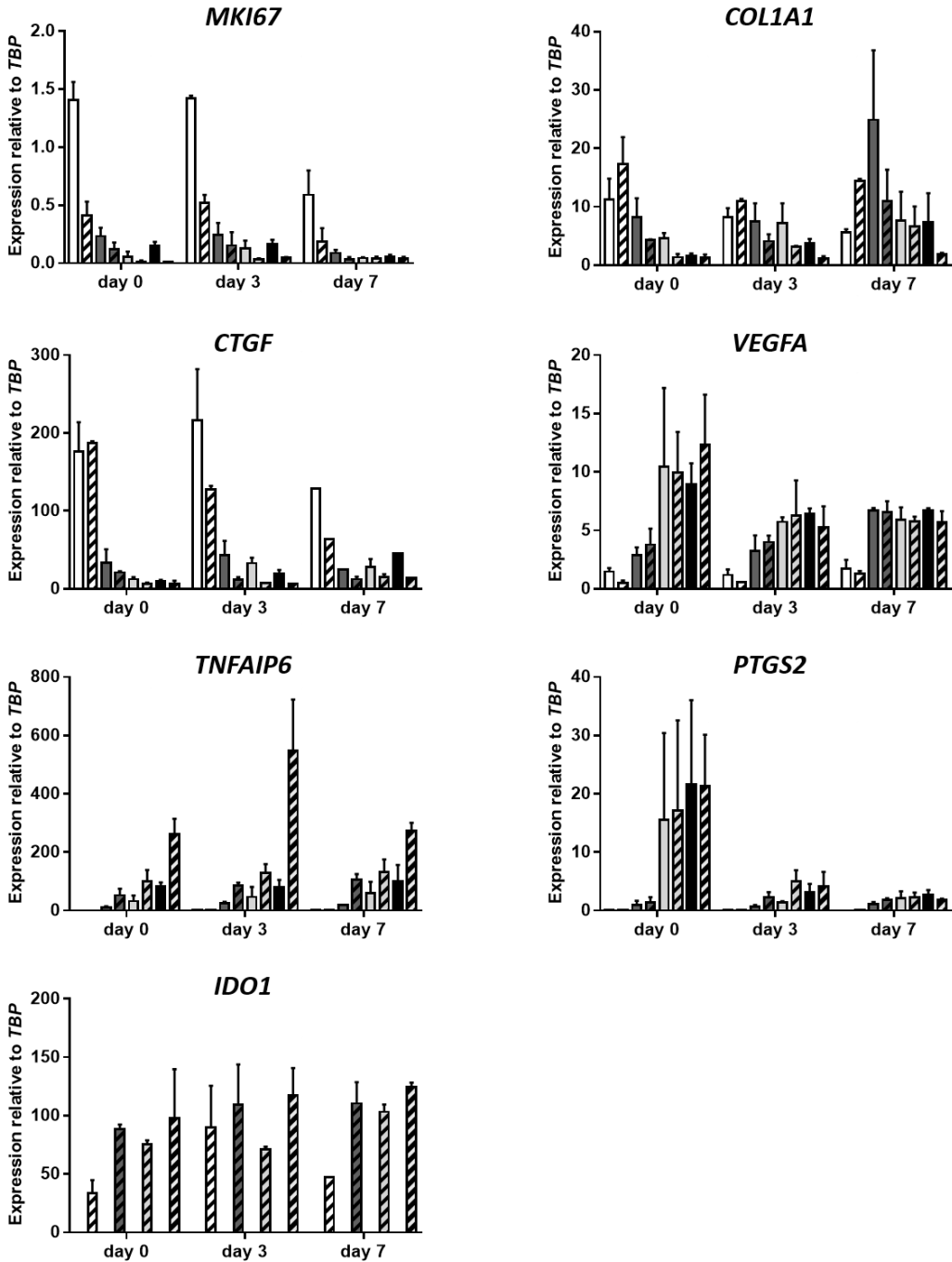
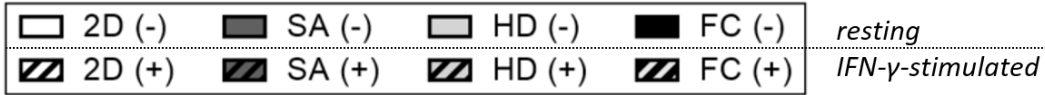


Supplementary Fig. S1. Time course of MSC aggregation by conventional methods.

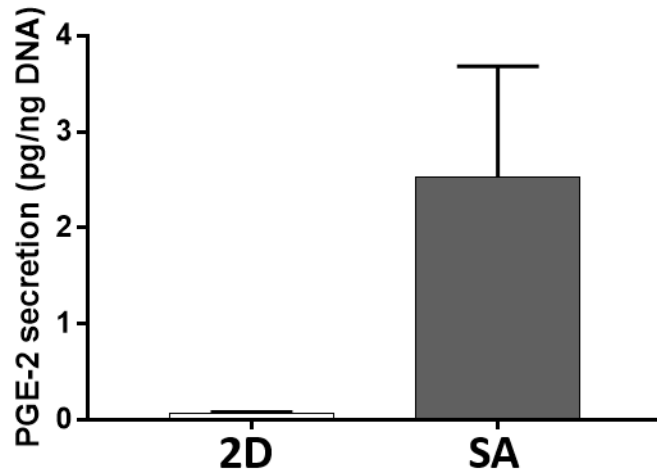
Brightfield images of MSCs in (A) HD and (B) FC formats from the time of seeding (0 hr) to 24 hr post-seed. Both methods generated three-dimensional structures by 6 hr post-seed, and formed compact aggregates by 24 hr. Compaction of HD and FC aggregates over time can be seen as changes in shape (oblong to spherical) and increased opacity from 6 hr to 24 hr.



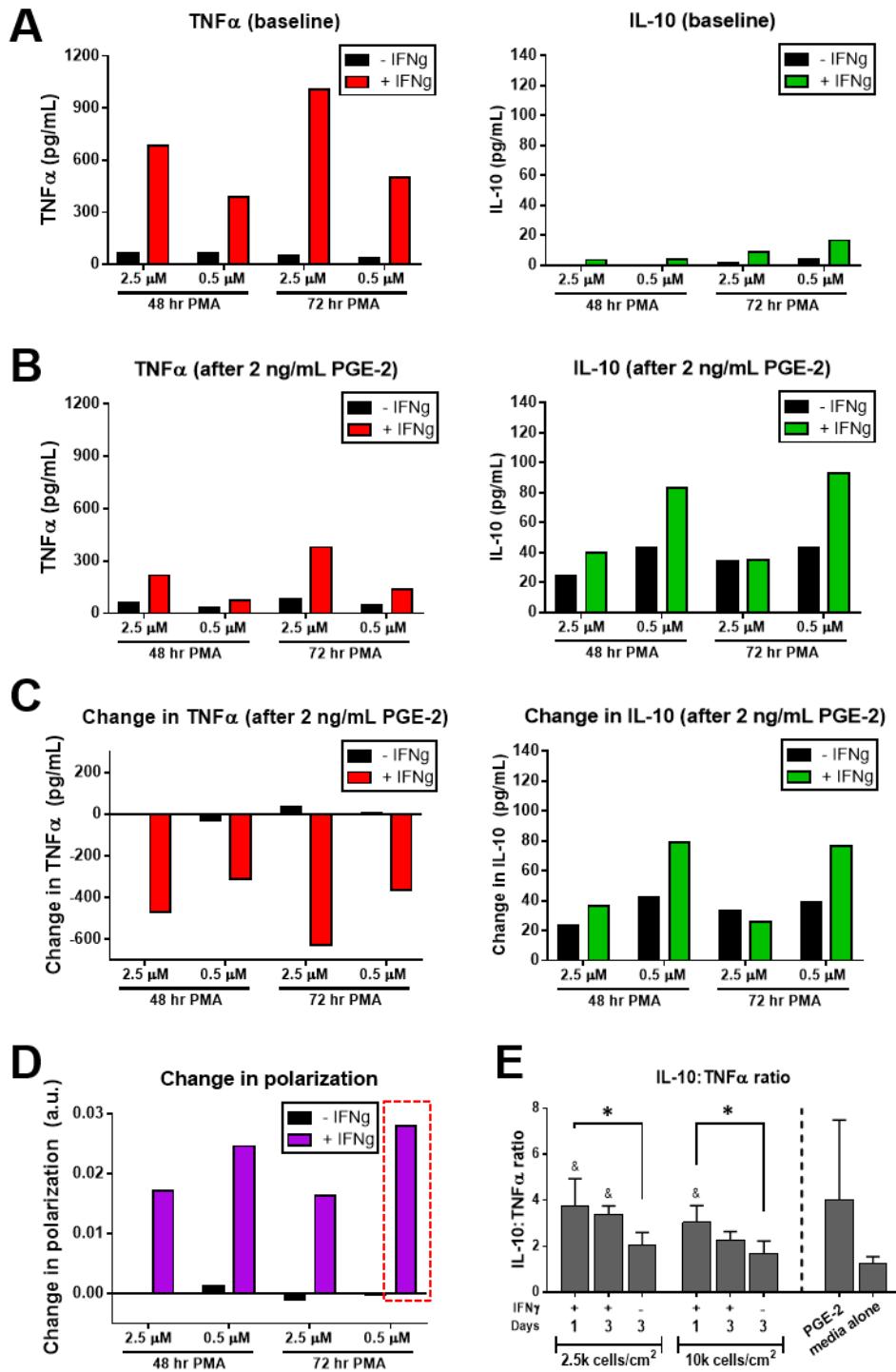
Supplementary Fig. S2. Trilineage differentiation capacity of 2D monolayer and 3D aggregate MSCs. 2D MSCs or 3D MSC aggregates (SA, HD, and FC) were plated on Collagen I-coated plates and maintained in (A) adipogenic, (B) chondrogenic, or (C) osteogenic differentiation media for 21 days before staining for Oil Red O, Alcian Blue, and Alizarin Red, respectively. Scale bars = 500 μ m.



Supplementary Fig. S3. Relative gene expression over time in resting or IFN- γ -stimulated MSCs cultured in 2D vs. 3D. Time course of expression for proliferation-, ECM-, pro-angiogenic, and immunomodulatory genes in 2D monolayer MSCs vs. SA, HD, and FC MSC aggregates.

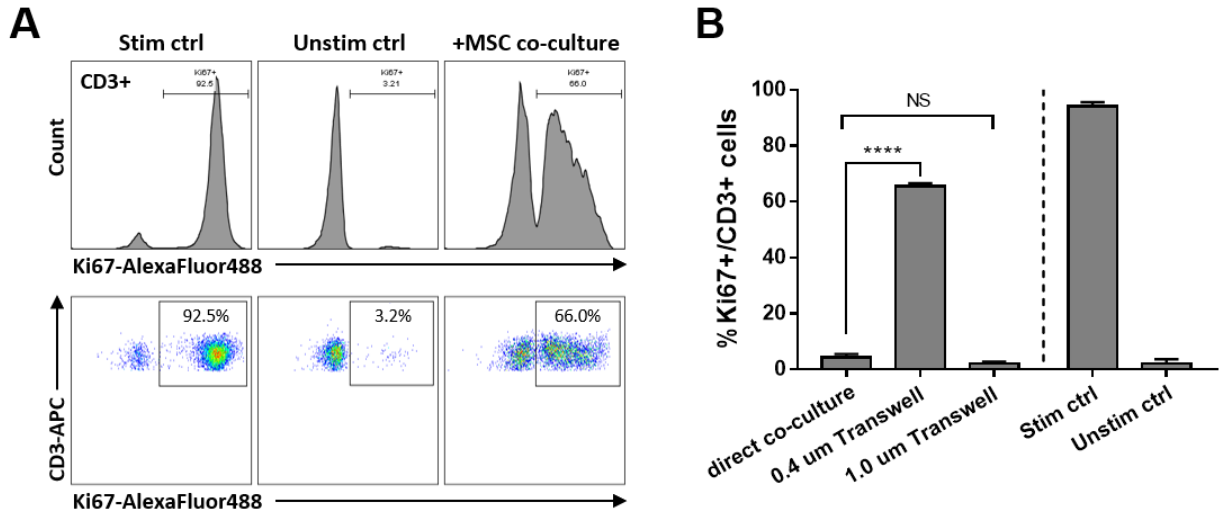


Supplementary Fig. S4. PGE2 production in 2D vs. 3D MSCs. MSCs in 3D aggregates (SA) produce >40-fold higher levels of PGE2 compared to 2D monolayer MSCs. PGE2 was measured in conditioned media from IFN- γ -stimulated MSCs.

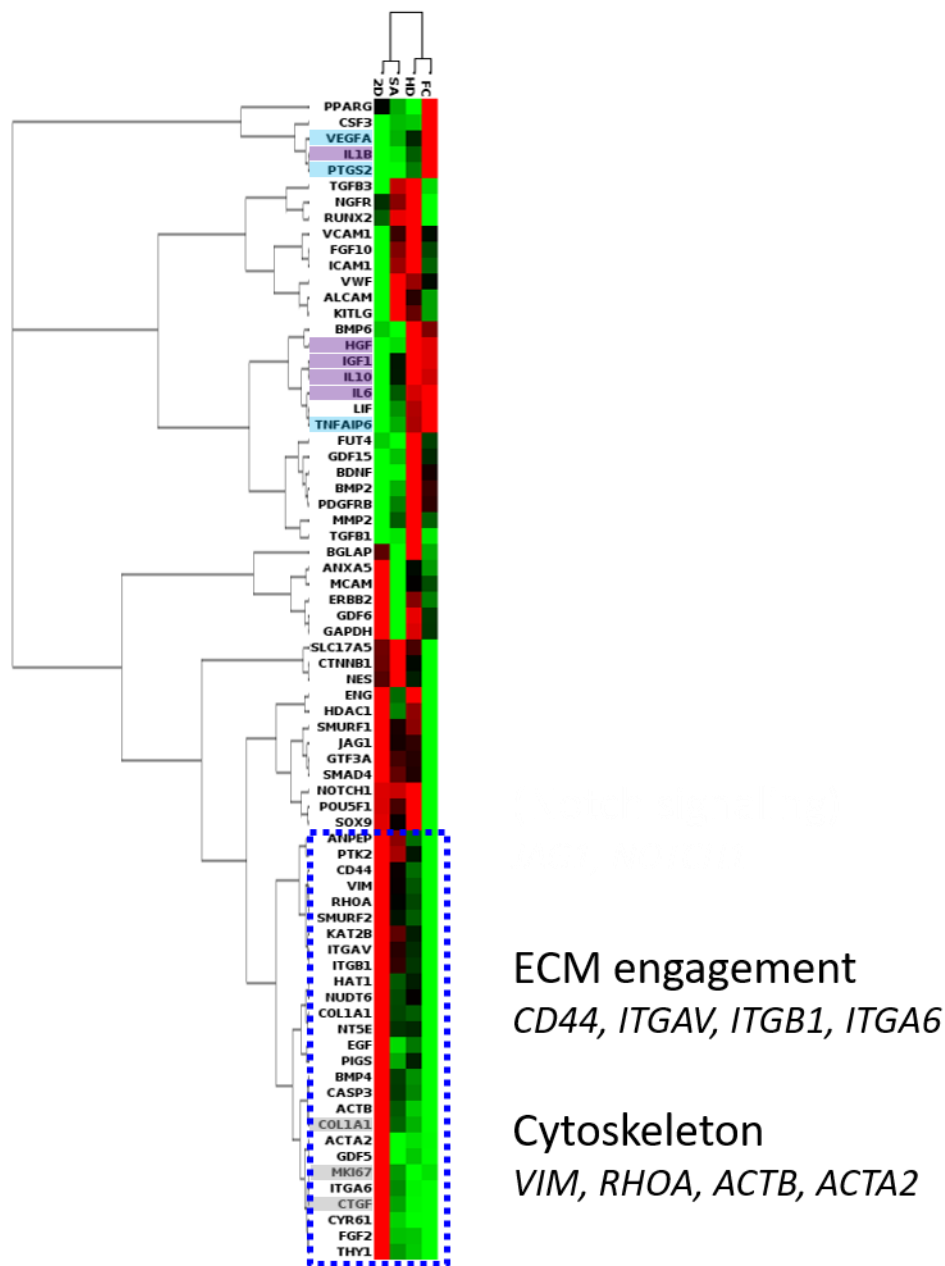


Supplementary Fig. S5. Development of macrophage polarization assay. (A) Baseline cytokine profile in M ϕ -CM following treatment (\pm IFNg) of PMA-treated THP-1s. (B) Cytokine profile in M ϕ -CM following additional treatment with 2 ng/mL PGE-2. (C) Change in cytokine profile in M ϕ -CM between baseline and PGE-2-treated M ϕ . (D) “Change in M ϕ polarization”, defined as a composite metric taking into account the differences in both TNF α and IL-10 production after PGE-2 treatment of M ϕ . Absolute changes in pg/mL secretion of each cytokine were weighted equally; decreases in TNF α production and increases in IL-10 production

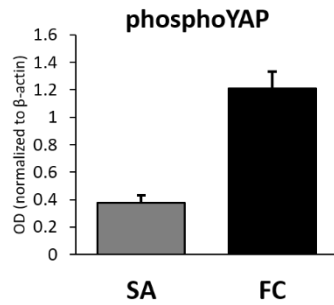
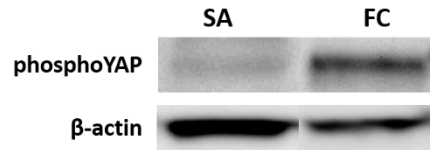
contributed positively to “change in polarization” metric. Red box denotes the treatment condition that was used for macrophage polarization assays. (E) Determination of cell number per media volume and duration (days) of MSC media conditioning for macrophage polarization assays. MSC media conditioning was performed with 2D MSCs in 12-well plate format ($2.5\text{k}/\text{cm}^2 = 4,500 \text{ cells/mL}$; $10\text{k}/\text{cm}^2 = 18,000 \text{ cells/mL}$). Graph shows IL-10:TNF α ratio in M ϕ -CM following treatment of macrophages with PGE-2 or media conditioned by IFN γ -stimulated or resting MSCs for 1 or 3 days. * indicates significant difference between denoted conditions. & denotes significant difference relative to negative control (“media alone”). $p < 0.05$



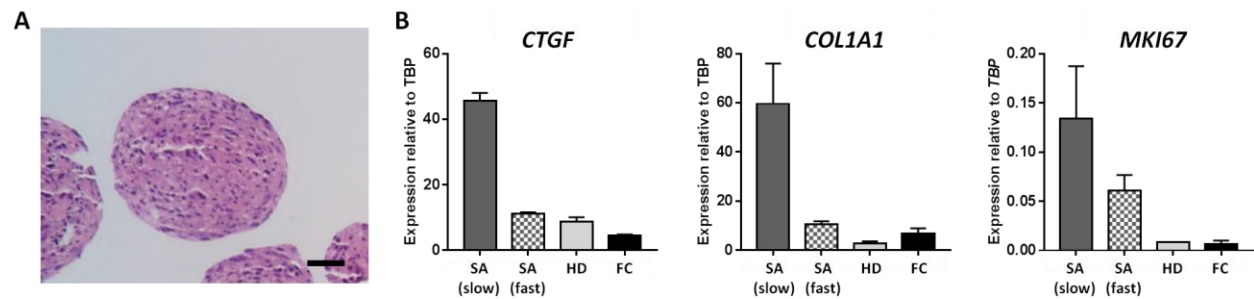
Supplementary Fig. S6. Refinement of T cell suppression assay. (A) Histogram representation of MSC-mediated suppression of T cell proliferation. (B) Effect of Transwell pore size on MSC suppression of T cell proliferation. 0.4 μm Transwell significantly reduces the capacity of 2D monolayer MSCs to suppress T cell proliferation, while 1.0 μm pore Transwell rescues the full suppressive effect of MSCs seen in direct co-culture. “Stim ctrl”: PBMCs activated by Suppression Inspector beads, no MSCs. “Unstim ctrl”: PBMCs without beads, no MSCs.



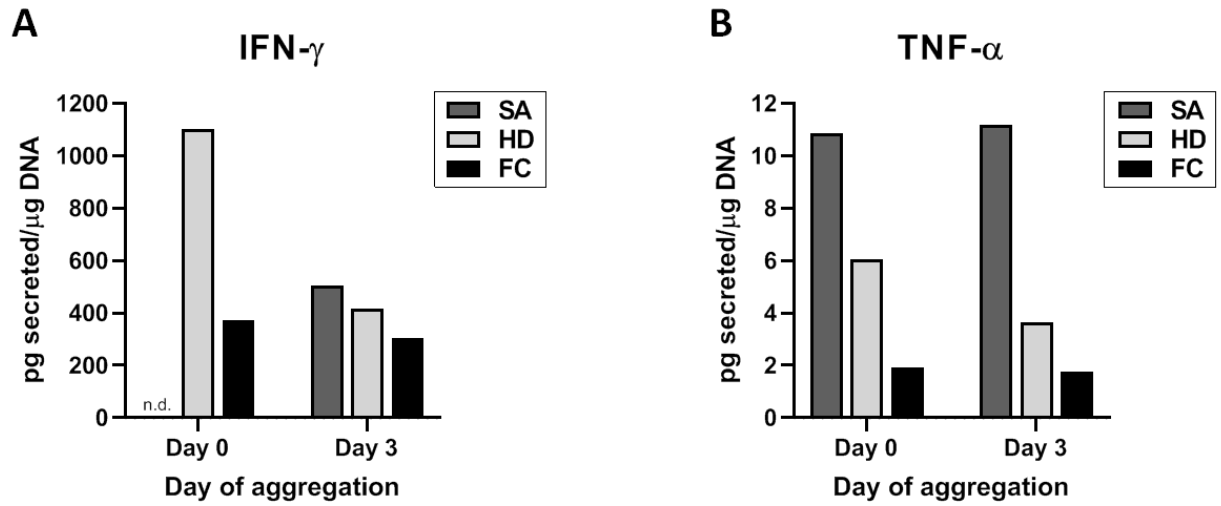
Supplementary Fig. S7. Unsupervised hierarchical clustering of MSC genes vs. culture format. Genes related to trophic/immunomodulatory factor production, cell-cell and cell-matrix interactions, cytoskeleton, and stemness/differentiation for 2D monolayer MSCs and 3D MSC aggregates generated by SA, HD, and FC methods were assessed by qPCR array at day 0 (resting conditions). Gene names highlighted in light blue and gray denote those that were assessed in time course studies in Fig. 3. Gene names in purple denote other common cytokines involved in immune regulation.



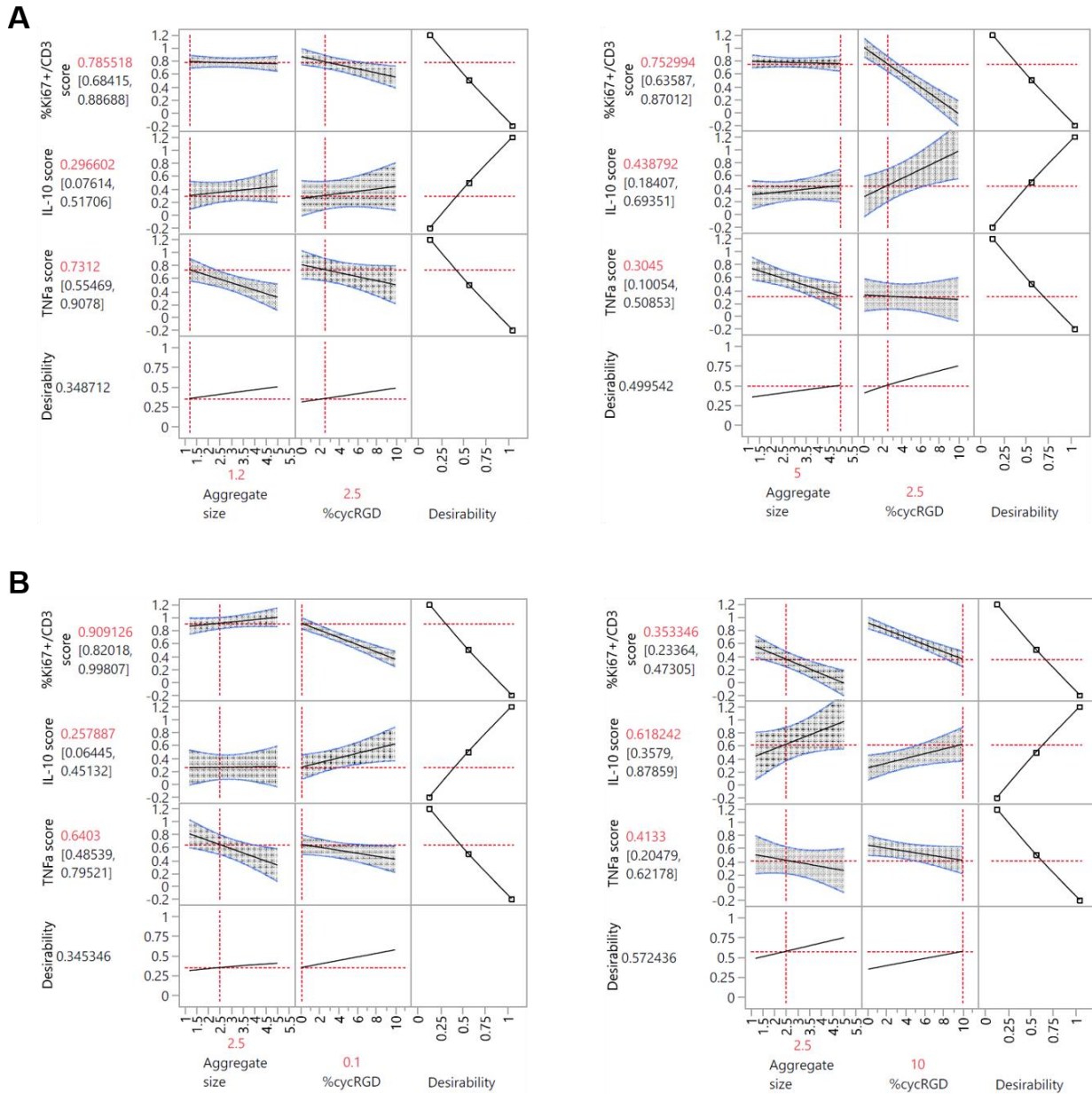
Supplementary Fig. S8. MSC aggregation method influences YAP phosphorylation. SA and FC MSC aggregates were formed by SA or FC methods and harvested for Western blot analysis at day 0 (72 hours after initial seeding). Western blots confirmed higher phosphoYAP levels in FC aggregates, indicative of decreasing YAP activity.



Supplementary Fig. S9. Faster aggregation kinetics downregulates expression of ECM- and proliferation-associated genes in SA aggregates. SA aggregates formed via “fast” self-assembly were generated from 0.5% cycRGDfC labile SAMs. (A) Representative H&E stain of day 0 “fast SA” MSC aggregates. Scale bar = 250 μ m. (B) Expression of ECM- and proliferation-associated genes in day 0 “fast SA” MSC aggregates, compared to other conditions tested in this study. Data shown are from experiments independent from those used to generate the data in Supplementary Fig. S2.



Supplementary Fig. S10. MSC aggregation method influences endogenous inflammatory cytokine production. Endogenous production of (A) IFN- γ and (B) TNF- α by SA, HD, and FC aggregates at Day 0 and Day 3 were measured from conditioned media (alphaMEM with 0.5% FBS) and normalized to total aggregate DNA. Cytokine production was measured using Inflammatory Cytokine Arrays (Raybiotech), while DNA was measured using Quant-iT PicoGreen dsDNA Assay Kit (Thermo Fisher Scientific). “n.d.” indicates signal was not detectable.



Supplementary Fig. S11. Extended model predictions from DOE model exemplify the interaction effect between aggregate size and aggregation kinetics. Prediction profiles showing effects of (A) Changing aggregate size while holding %cycRGD constant and (B) Changing aggregation kinetics (%cycRGD) while holding aggregate size constant. The DOE model identified an interaction effect between aggregate size and kinetics in their influence on %Ki67+/CD3 score.